

Growth of fingerlike protrusions driven by molecular motorsK. Kruse^{1,2,*} and K. Sekimoto^{1,3}¹*Institut Curie, Physicochimie, UMR CNRS/IC 168, 26 rue d'Ulm, 75248 Paris Cedex 05, France*²*Max-Planck-Institut für Strömungsforschung, Bunsenstrasse 10, D-37073 Göttingen, Germany*³*Non-Equilibrium Section, Yukawa Institute, Kyoto University, Kyoto 606-8502, Japan*

(Received 1 February 2002; revised manuscript received 23 May 2002; published 19 September 2002)

The actin cortex is an important part of the motile machinery of a eucaryotic cell. The cortex is steadily reorganized, for example, through the action of molecular motors forming active crosslinks between pairs of actin filaments. Here, the effect of correlations between molecular motors on the induced relative motion of two aligned filaments is investigated. It is found that the average relative velocity between filaments depends nonmonotonically on the motor concentration. Depending on the properties of the filaments' ends, the active interaction between filaments of the same orientation may lead either to a complete overlap or to separation. In addition to pure actin polymerization the active separation of filaments might be involved in the growth of long fingerlike protrusions (filopods).

DOI: 10.1103/PhysRevE.66.031904

PACS number(s): 87.16.Qp, 87.16.Ka, 45.50.Jf

I. INTRODUCTION

During the growth of an axon, nerve cells extend fingerlike protrusions a tenth of a micron wide and up to 50 μm long [1]. These so-called filopods are formed by a bundle of long filamentous polymers made of the protein actin. Due to different polymerization rates, the two ends of actin filaments can be distinguished. The bundle of actin filaments in a filopod is oriented such that the faster polymerizing plus ends point towards the tip, while the minus ends point towards the cell body. Therefore, polymerization of actin has been assumed to provide the driving force for growing these protrusions.

Indeed, polymerization of actin is very likely to be the driving force in several mechanisms of cell motility [2]. For example, the bacterium *Listeria monocytogenes* advances by growing an actin comet at one of its poles and the leading edge of moving eucaryotes is a place of intense actin polymerization. Recently, *in vitro* experiments have been conceived in order to investigate if actin polymerization alone is sufficient to drive these processes. For *Listeria* this is the case, as latex beads immersed in an extract containing only proteins, that are involved in the polymerization of actin, may grow a comet and move [3]. Concerning the growth of filopods, polymerization of actin within giant vesicles has been found to produce fingerlike protrusions [4]. However, an unphysiologically high concentration of monomeric actin seems to be necessary. Furthermore, the protrusions generated in this way extended only up to a length of about 10 μm .

Also on theoretical grounds there are indications that in addition to pure actin polymerization there is another mechanism involved in the growth of long filopods. The current understanding of how polymerization of actin may push a membrane states that fluctuations of the membrane or bending fluctuations of actin filaments close to the membrane

provide the necessary space needed for further polymerization [5,6]. Within this framework indications of fingerlike protrusions have been reported only in the case of a fluctuating membrane [7]. Membrane fluctuations are, however, likely to be suppressed at the tip of filopods due to membrane proteins accumulated at this point [6]. Here, we present a possible mechanism for filopod growth, based on the action of molecular motors accompanying the polymerization of actin.

Molecular motors are ATPases, i.e., proteins catalyzing the hydrolysis of ATP, that undergo a series of conformational changes during the hydrolysis of ATP [1]. On an appropriate substrate, these conformational changes induce a displacement of the motor relative to the substrate. For example, motors of the myosin superfamily advance on an actin filament towards the filament's plus end. In the last 10–15 years, motor proteins have been intensively studied in order to elucidate the mechanism by which an individual motor moves forward. See [8,9] for reviews of the current experimental and theoretical understanding. More recently, collective properties of filament-motor systems start to attract a broader interest. Collective effects in these systems appear, because motors or complexes of motors may actively crosslink filament pairs, resulting in an active relative displacement of the filaments. As a consequence, contraction of filament bundles followed by filament sorting [10] has been observed, as well as the formation of asters, vortices, and networks of filaments [11,12] in a quasi-two-dimensional geometry. Theoretically, filament sorting [13], contraction of disordered filament bundles [14,15], and persistent filament transport [16] have been obtained.

In this work we will look at the influence of correlation effects between motors due to excluded volume interactions on the relative motion between two actively cross-linked aligned filaments. We will first study the case when the unbound motors are homogeneously distributed around the filaments. Remarkably, due to the motor interactions, filaments of the same orientation will under certain conditions tend to separate from each other. This observation suggests a mechanism of filopod growth by pushing a filament against the tip.

*Present address: Max-Planck-Institut für Physik komplexer Systeme, Nöthnitzer Str. 38, D-01187 Dresden, Germany.

In the last section, we investigate this possibility more closely.

II. A MODEL FOR MOTOR-INDUCED SLIDING OF FILAMENTS

Let us start by describing the general setting, which we will use in the following sections. It is chosen so that it captures the qualitative features of the motor-filament interactions, but neglects details, many of which are still unknown. A filament is represented as a linear lattice composed of L equally spaced sites, with site number 1 being associated with the filament's minus end and site number L with its plus end. Molecular motors bound to the filament are represented as particles occupying the sites of the corresponding lattice. Here, each site accepts at most one motor and the actual state of site number i is given by the value of s_i , which is 0 for an empty site and 1 otherwise. Two filaments are displaced with respect to each other by a molecular motor—or a compound of motors—if this motor is bound to both filaments simultaneously and advances on one of them. The current of motors from site i to site $i+1$ is denoted by j_i and has the dimension of an inverse time (number of motors advancing from i to $i+1$ per unit time).

The expectation values $S_i \equiv \langle s_i \rangle$ and $J_i \equiv \langle j_i \rangle$ are calculated by using the following model for a motor moving along a single filament. A motor on site i may advance towards the plus end of a filament by hopping to site $i+1$, provided that this site is empty. Within an interval of time Δt , the probability for such a hopping event is $\omega_h \Delta t$, such that $J_i = \omega_h \langle s_i (1 - s_{i+1}) \rangle$. Apart from hopping, motors may attach to and detach from the filament at any site. The corresponding rates are denoted by ω_a and ω_d , respectively. The last site of the filament requires special consideration for there is no further site the motor may hop to. We assume that the detachment rate at this site is given by $\omega_d + \omega_h (1 - \sigma)$ with $\sigma \leq 1 + \omega_d / \omega_h$. Note, that the attachment rate ω_a will in general not be equal for all sites along the filament as it depends on the amount of unbound motors present in the environment of these sites. If ω_a were different from zero only on the first site and $\omega_d = 0$, then this model is the totally asymmetric exclusion model [17]. Putting everything together, the time evolution of the average occupation number S_i of site i is given by

$$\begin{aligned} \frac{d}{dt} S_i = & \omega_h S_{i-1} (1 - S_i) - \omega_h S_i (1 - S_{i+1}) \\ & + \omega_a (1 - S_i) - \omega_d S_i, \end{aligned} \quad (1)$$

where we have used the mean field approximation $\langle s_i s_{i+1} \rangle = S_i S_{i+1}$. The boundary conditions are $S_0 = 0$ and $S_{L+1} = \sigma$.

In order to calculate the average velocity between two aligned filaments, denoted by 1 and 2, we make the following assumptions: Firstly, a motor can only connect the two filaments at two adjacent sites. Secondly, filaments are taken to be rigid objects. Finally, the probability of forming a crosslink is weak enough such that it suffices to consider

configurations of one crosslink per pair only. Let the crosslinking motor be on site i of filament 1 and on site k of filament 2. Then, within an interval of time Δt , the probability for a relative displacement between the two filaments due to the motor advancing on filament 1 is $\omega_h (1 - s_{i+1}^{(1)}) \Delta t$, where $s_i^{(k)}$ is the occupation number of site i on filament k . An analogous expression holds if the motor advances on filament 2. A crosslink between the two filaments is assumed to be established with probability p_{cl} if two facing sites on these filaments are occupied. The value of p_{cl} is assumed to be constant along the filaments, but will, in general, depend on their relative orientation. For the average velocity of filament 2 relative to filament 1 in units of monomers per time we thus obtain in the stationary state

$$v = \sum_{(i,k) \in \Delta} p_{cl} \omega_h \langle j_i^{(1)} s_k^{(2)} \pm s_i^{(1)} j_k^{(2)} \rangle. \quad (2)$$

Here, Δ denotes the region of overlap of the two aligned filaments, (i,k) are pairs of adjacent sites on the different filaments, $j_i^{(k)}$ is the current from site i to site $i+1$ on filament k , and $\langle \dots \rangle$ denotes the ensemble average. The plus sign applies in the case of antiparallel filaments, i.e., filaments of opposite orientation, the minus sign in the opposite case of parallel filaments.

In order to calculate the needed expectation values, we will use the independent filaments approximation

$$\omega_h \langle s_i^{(1)} s_k^{(2)} (1 - s_{i+1}^{(1)}) \rangle = J_i^{(1)} S_k^{(2)}. \quad (3)$$

Thereby, everything can be calculated using expectation values obtained for single filaments. This approximation is appropriate if, for example, motors have to form a compound in order to cross-link two filaments and if these compounds form rarely and are short-lived compared to typical time scales for the dynamics on a filament. We can give another example: let there be two kinds of motors showing both the same dynamics on a single filament, but only motors of *one* type are able to cross-link filament pairs. Then the approximation is appropriate under the condition of only a few crosslinkers.

III. FILAMENT SLIDING FOR A HOMOGENEOUS DISTRIBUTION OF UNBOUND MOTORS

In this section we will study the case of a spatially constant attachment rate ω_a , corresponding to homogeneously distributed unbound motors. Only the stationary states will be considered.

Let us first briefly discuss the motor dynamics on one filament. If motors are incapable of advancing along the filament, i.e., $\omega_h = 0$, the mean occupation of any site is given by $r \equiv \omega_a / (\omega_a + \omega_d)$. The same holds for all values of ω_h if the filament is of infinite length or forms a closed loop. In the case of a finite filament length with open boundaries, the distribution changes as ω_h is increased from zero to a finite value. Here, with increasing ω_h , the homogeneous distribution is changed from the boundaries towards the bulk. Our numerical analysis shows that this is mostly effective in the

case of $r < 1/2$. For $r > 1/2$, the current towards the plus end dominates, and little influence of the boundary at $i=L$ is observed except for the very neighbors of the boundary. A simple analytical analysis also supports this result (not shown).

Towards the minus end, the filament is on average less populated, as motors cannot arrive in this region by moving on the filament. Concerning the behavior towards the plus end we have to distinguish two cases. If $\sigma > r$, then detachment from the last site is less likely than in the bulk. Consequently, motors jam and this region is more densely occupied than the bulk. In the opposite case $\sigma < r$, the mean occupation correspondingly diminishes towards the plus end. See Fig. 1, which presents the mean occupation number in the steady state as obtained by a numerical simulation of the stochastic motor dynamics.

This figure also represents the average motor current. Starting from the minus end, it grows from zero up to its bulk value $\omega_h r(1-r)$. For $\sigma > r$ it then decreases towards the plus end as a consequence of jamming. In the opposite case, on the contrary, it increases as there are on average more free sites available.

We will now investigate the relative velocity between two aligned filaments of a common length L . To this end we calculate the velocity of filament 2 in a frame of reference associated with filament 1. The orientation of filament 1 is chosen so that its plus end points into the direction of in-

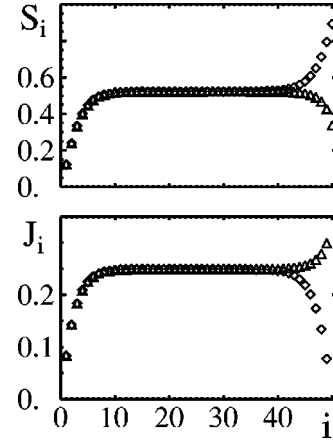


FIG. 1. The steady state for motors moving on one filament. Shown are the mean occupation number S_i (top) and the mean current $J_i \equiv \langle j_i \rangle / \omega_h$ (bottom) along the filament for $\omega_a / \omega_h = 0.1$, $\omega_d / \omega_h = 0.1$, and $L = 50$. Diamonds are for $\sigma = 1$, triangles for $\sigma = 0$.

creasing x . Using the independent filaments approximation (3), the distinction between the mean occupation number of filaments 1 and 2 in Eq. (2) is no longer needed. The same holds for the currents. As a function of the distance ξ between the filaments' minus ends, we obtain for the relative velocity of parallel filaments, which overlap if $\xi = -L + 1, \dots, L - 1$,

$$v^{(\text{pa})}(\xi) = \begin{cases} \text{sgn}(\xi) p_{\text{cl}} \left[\sum_{i=1}^{L-\xi-1} J_{i+\xi} S_i - \sum_{i=1}^{L-\xi} J_i S_{i+\xi} \right] & \text{for } \xi = \pm 1, \dots, \pm(L-1), \\ 0 & \text{for } \xi = 0. \end{cases} \quad (4)$$

Here, $\text{sgn}(\xi)$ is 1 for $\xi > 0$ and -1 otherwise. Filaments of opposite orientation overlap if $\xi = 0, \dots, 2L - 2$ and their average relative velocity is given by

$$v^{(\text{ap})}(\xi) = 2p_{\text{cl}} \begin{cases} \sum_{i=1}^{1+\xi} J_i S_{2+\xi-i} & \text{for } \xi = 0, \dots, L-2, \\ \sum_{i=\xi-L+2}^{L-1} J_i S_{2+\xi-i} & \text{for } \xi = L-1, \dots, 2L-3. \end{cases} \quad (5)$$

The induced sliding between parallel filaments is a boundary effect. Even if motors did not interact among themselves, i.e., if $j_i = \omega_h s_i$, finite size effects would lead to a non-vanishing average velocity. The filaments would then always tend to increase their overlap. Numerical investigation of the stochastic dynamics for interacting motors reveals, however, that for $\sigma = 0$ and intermediate values of ω_h / ω_a , filaments of the same orientation tend to repel each other. See Fig. 2 which presents the average filament velocities as a function of their overlap for two different values of ω_a , i.e., two different motor densities. Note that filaments repel each other, when $v^{(\text{pa})}$ has the same sign as ξ . For $\omega_h \ll \omega_a$ and for $\omega_h \gg \omega_a$ parallel filaments will increase their overlap as in

the case of noninteracting motors. However, the average velocity may significantly increase due to the motor interactions.

For antiparallel filaments, the motors are in all cases increasing the distance between the filaments' minus ends. Since, in contrast to the motion of parallel filaments, motor-induced sliding of antiparallel filaments is a bulk effect, the relative velocity depends only weakly on the value of σ . A simple estimate for $v^{(\text{ap})}$ is given by $2p_{\text{cl}} \omega_h r^2 (1-r)$ times the overlap of the two filaments.

In order to compare the values for different ω_a , corresponding to different numbers of unbound motors, let us define the following average relative velocities:

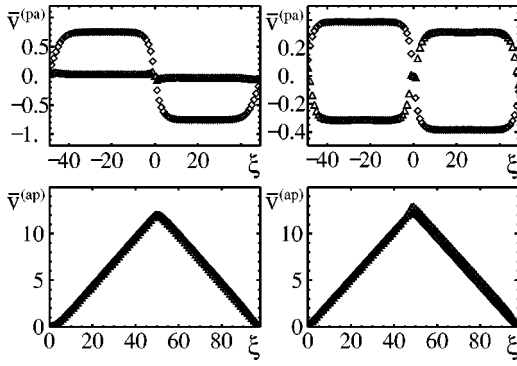


FIG. 2. Relative velocities between two aligned filaments of common length as a function of their minus end distance. The top panels show $\bar{v}^{(pa)} \equiv v^{(pa)}/(2p_{cl}\omega_h)$ for parallel filaments, the bottom panels $\bar{v}^{(ap)} \equiv v^{(ap)}/(2p_{cl}\omega_h)$ for antiparallel filaments. Left panels are for $\omega_a/\omega_h=0.1$, while right panels are for $\omega_a/\omega_h=0.4$. Furthermore, $\omega_d/\omega_h=0.1$ and $L=50$. Diamonds are for $\sigma=1$, triangles for $\sigma=0$.

$$V^{(pa)} = \frac{2}{2L-1} \sum_{\xi=1}^{L-1} v^{(pa)}(\xi) \quad (6)$$

for parallel filaments and

$$V^{(ap)} = \frac{1}{2L-1} \sum_{\xi=0}^{2L-3} v^{(ap)}(\xi) \quad (7)$$

for antiparallel filaments. Figure 3 presents the average relative velocities $V^{(pa)}$ and $V^{(ap)}$ for attachment rates corresponding to bulk occupation numbers in the range of about 0.1 to 0.9. The average relative velocity for parallel filaments initially decreases with ω_a , until it increases around $\omega_a \approx \omega_d$. For $\sigma=0$ it then changes sign and will asymptotically approach 0. In the case $\sigma=1$ the average velocity $V^{(pa)}$ is negative for all values of ω_a , but also approaches zero in the limit $\omega_a \rightarrow \infty$. The average velocity of antiparallel filaments is reasonably approximated using the rough estimate presented in the previous paragraph, as is shown in the figure. In

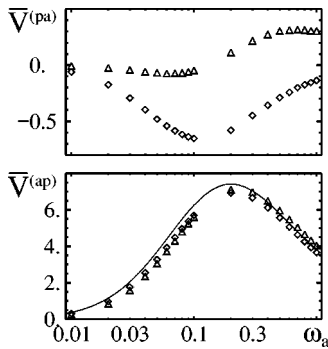


FIG. 3. Average relative velocities between two aligned filaments of common length as a function of ω_a/ω_h . The top panel shows $\bar{V}^{(pa)} \equiv V^{(pa)}/(2p_{cl}\omega_h)$, the bottom panel $\bar{V}^{(ap)} \equiv V^{(ap)}/(2p_{cl}\omega_h)$. The remaining parameters are $\omega_d/\omega_h=0.1$, $L=50$, and $\sigma=1$ (diamonds) or $\sigma=0$ (triangles). The solid line is obtained from the estimate indicated in the text.

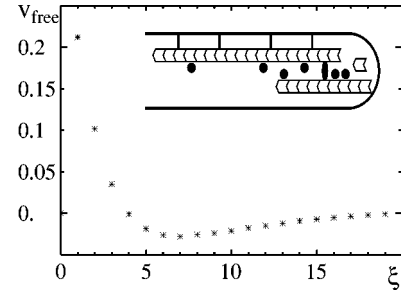


FIG. 4. Relative velocity between two aligned filaments for an exponential distribution of unbound motors in units of sites per unit time and divided by $p_{cl}\omega_h$. The parameters are $\omega_d^0/\omega_h=0.1$, $\omega_d/\omega_h=0.1$, and $\lambda=10$. The free filament is of length $L=20$ and has $\sigma=1$, while for the attached filament $L=50$ and $\sigma=0$. The inset shows a schematic representation of the growth mechanism. Motors are represented as dots, the cross-linking motor as an ellipse. Only bound motors are represented. Bars indicate the attachment of one filament to the substrate.

this approximation the maximal velocity is attained for $\omega_a = 2\omega_d$, corresponding to a bulk mean occupation of $r = 2/3$. Let us close this section with the remark that for $\sigma = 1$, both average velocities, $V^{(pa)}$ and $V^{(ap)}$, were found to decrease with increasing ω_h .

IV. A MOTOR-DRIVEN MECHANISM FOR FILOPOD GROWTH

Based on the observation of separating parallel filaments, we propose the following mechanism for filopod growth, as illustrated in the inset of Fig. 4. Recall that a filopod contains a bundle of actin filaments, all oriented with their plus ends outwards. Suppose that some of these filaments are attached to a substrate, while other filaments are free to move along their axis. Motion in the perpendicular directions are suppressed by the cell membrane. As found above, through the action of molecular motors, the free filaments will under appropriate conditions be transported into the direction of their plus ends. Thereby they might push the membrane away from the plus ends of the attached filaments, such that the latter are thus able to polymerize. In the following we show that there is a stable state of continuous actin polymerization.

Consider the simple situation of two filaments only, one of which is attached to a substrate and long, while the other is short and free to move along its axis. In a filopod, motors are nonhomogeneously distributed as they are moving on the filaments towards the tip. For simplicity we will suppose a distribution of free motors decreasing exponentially from the tip towards the cell body [18]. In our model this distribution of unbound motors translates into an attachment rate ω_a which decreases exponentially from the membrane, $\omega_a(i) = \omega_a^0 \exp(-i/\lambda)$, where i is the distance to the membrane. For a filament with its plus end next to the membrane, we choose $\sigma=1$, i.e., at the plus end, a motor cannot leave the filament by hopping off the filament. For a filament with its plus end away from the membrane we choose $\sigma=0$.

Let us first calculate the average velocity v_{free} of the free filament as a function of the distance from its plus end to the

plus end of the attached filament. We choose a frame such that the origin associated with the plus end of the attached filament and such that the plus ends points into the direction of positive x . A typical result for positive ξ is shown in Fig. 4. Here, ξ is the position of the free filament's plus end. Up to a distance of a few monomers, the velocity of the free filament is positive, corresponding to separation of the filaments. The velocity then changes its sign. Such a change in sign is not observed in the case of spatially constant ω_a . The critical distance, for which the velocity changes its sign, grows with increasing λ . Note that this stationary point is stable, as the velocity is positive before this point and negative beyond.

As long as the plus end of the attached filament is sufficiently far apart from the membrane, further actin monomers may attach to this end. We denote the polymerization rate by ω_{pol} and the length of a monomer by ℓ , where this length is less than or equal to the step size of a motor. Then the plus end will on average advance with respect to the substrate with velocity $v_{\text{pol}} = \omega_{\text{pol}}\ell$. In the frame associated with the attached filament's plus end the velocity of the free filament is thus reduced by v_{pol} . As long as the polymerization velocity is not too big, a stationary state will still exist for $\xi > 0$. It is stable and corresponds to persistent growth of the filopod. Note that the growth velocity of the filopod would then be v_{pol} .

For $\xi < 0$, i.e., when the plus end of the attached filament is to the left of the attached filament's plus end, the velocity of the free filament is negative in the case $v_{\text{pol}} = 0$. Now that its plus end is some distance apart from the membrane, it may polymerize. Depending on the relation of the polymerization velocity and the active velocity induced by the motors, the free filament will either be transported towards the cell body or grow until its plus end reaches the membrane and a fluctuation may again induce filopod growth.

V. CONCLUSION

In conclusion, we have investigated the effects of excluded volume interactions between molecular motors on the motor-induced sliding velocity between aligned filaments. For both parallel and antiparallel filaments, we have found a nonmonotonic dependence of this velocity on the motor concentration. Under appropriate conditions, the velocity between parallel filaments was seen to change sign as a consequence of the motor interactions. Instead of increasing their overlap, as is the case for noninteracting motors, the filaments then repel each other. A way to experimentally study the active interaction between aligned filaments *in vitro* would be through the use of microstructured surfaces.

Filament separation driven by molecular motors could be used in order to push an object. As we have argued, a possible application in biological cells is the growth of fingerlike protrusions containing a bundle of parallel actin filaments. If collective effects between molecular motors are important in this process, then changing their concentration in a protrusion should influence the final length of the filopod. Our calculations indicate that initially this length should grow with the motor concentration and then decrease again. A more realistic description of this situation would, however, require taking situations into account in which filaments are cross-linked by more than one motor, which is beyond the scope of the present work.

ACKNOWLEDGMENTS

One of the authors (K.S.) thanks the colleagues of the Curie Institute and the CNRS for financial support to study there. K.K. acknowledges support by the Max-Planck-Gesellschaft.

-
- [1] B. Alberts *et al.*, *Molecular Biology of the Cell*, 3rd ed. (Garland, New York, 1994).
 - [2] G.G. Borisy and T.M. Svitkina, *Curr. Opin. Cell Biol.* **12**, 104 (2000).
 - [3] T.P. Loisel *et al.*, *Nature (London)* **401**, 613 (1999).
 - [4] H. Miyata *et al.*, *Proc. Natl. Acad. Sci. U.S.A.* **96**, 2048 (1999).
 - [5] C. Peskin, G. Odell, and G. Oster, *Biophys. J.* **65**, 316 (1993).
 - [6] A. Mogilner and G. Oster, *Biophys. J.* **71**, 3030 (1996).
 - [7] A. Mogilner and G. Oster, *Eur. Biophys. J.* **25**, 47 (1996).
 - [8] See the special issue on molecular motors in *Philos. Trans. R. Soc. London, Ser. A* **355**, 1396 (2000).
 - [9] F. Jülicher, A. Ajdari, and J. Prost, *Rev. Mod. Phys.* **69**, 1269 (1997).
 - [10] K. Takiguchi, *J. Biochem.* **109**, 502 (1991).
 - [11] F.J. Nédélec *et al.*, *Nature (London)* **389**, 305 (1997).
 - [12] T. Surrey *et al.*, *Proc. Natl. Acad. Sci. U.S.A.* **95**, 4293 (1998).
 - [13] H. Nakazawa and K. Sekimoto, *J. Phys. Soc. Jpn.* **65**, 2404 (1996).
 - [14] K. Sekimoto and H. Nakazawa, in *Current Topics in Physics*, edited by Y. M. Cho, J. B. Hong, and C. N. Yang (World Scientific, Singapore, 1998), Vol. 1, p. 394; K. Sekimoto and H. Nakazawa, e-print physics/0004044.
 - [15] K. Kruse and F. Jülicher, *Phys. Rev. Lett.* **85**, 1778 (2000).
 - [16] K. Kruse, S. Camalet, and F. Jülicher, *Phys. Rev. Lett.* **87**, 138101 (2001).
 - [17] B. Derrida and M. R. Evans, in *Nonequilibrium Statistical Mechanics in One Dimension*, edited by V. Privman (Cambridge University Press, Cambridge, England, 1997), Chap. 14.
 - [18] F. Nédélec, T. Surrey, and A.C. Maggs, *Phys. Rev. Lett.* **86**, 3192 (2001).